

Electronic Supplementary Information for

Anodic Substitution Reaction of Carbamates in a Flow Microreactor Using a Stable Emulsion Solution

Rio Mikami, Yuto Nakamura, Naoki Shida and Mahito Atobe**

Department of Engineering and Science, Yokohama National University

79-5 Tokiwadai, Hodogaya-ku, Yokohama, Kanagawa, Japan.

Tel: + 81- 45-339-4214; Fax: +81-45-339-4214

E-mail: atobe@ynu.ac.jp (M.A.); shida-naoki-gz@ynu.ac.jp (N.S.)

Contents

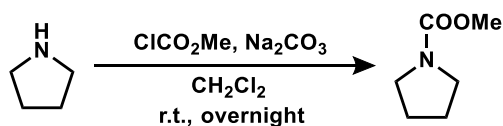
1. <i>General consideration</i>	S2
2. <i>Synthesis</i>	S2
3. <i>Preparation of emulsion solutions</i>	S7
4. <i>Fabrication of a flow microreactor</i>	S8
5. <i>Linear sweep voltammetry</i>	S9
6. <i>General procedure for electrolysis in the two-phase emulsion system using the flow microreactor</i>	S9
7. <i>Procedure for electrolysis in the one-phase system using the flow microreactor</i>	S10
8. <i>Procedure for electrolysis in the two-phase emulsion system using the batch type reactor</i>	S10
9. <i>Linear sweep voltammograms for the oxidation of substrate 1, allyl-TES, and product 2 in the one-phase system</i>	S11
10. <i>Stability of an allyl-TES emulsion solution prepared by tandem acoustic emulsification</i>	S12
11. <i>Electrolysis in the two-phase emulsion system using the flow microreactor at various experimental parameters</i>	S13
12. <i>Effect of emulsification conditions on the stability of emulsions</i>	S17
13. <i>Linear sweep voltammograms of allyl-TES in the two-phase emulsion system prepared by various emulsification conditions</i>	S18
14. <i>Linear sweep voltammograms of various allyl nucleophiles in the one-phase system</i>	S19
15. <i>Size distribution and average diameter of emulsion droplets of various allyl nucleophiles</i>	S20
16. <i>Linear sweep voltammograms of various allyl nucleophiles in the two-phase emulsion system</i>	S21
17. <i>Effect of the allyl nucleophiles on current efficiency for the detectable products</i>	S22
18. <i>Effect of the presence of various carbamates on the allyl-TES emulsion droplets</i>	S23
19. <i>GC analysis</i>	S24
20. <i>¹H NMR spectra</i>	S30
21. <i>Supporting reference</i>	S35

1. General consideration

1-Ethyl-3-methylimidazolium tetrafluoroborate ([EMIM][BF₄]) purchased from Ionic Liquids Technologies GmbH was mixed with granular activated carbon and stirred overnight. The mixture was filtered through a syringe filter (MS Glass Fiber Syringe Filter, Membrane Solutions) and dried for 2 hours using a vacuum pump. Carbamates (**1**, **5**, and **7**), α -allylated products (**2**, **4**, **6**, and **8**), and by-products were synthesized according to the reported procedure.¹⁻³ The rest of the reagents and solvents were purchased from commercial sources and used without further purification. Gas chromatography (GC) analyses were performed using a Shimadzu gas chromatograph (GC2014) equipped with a Tween 80 (3 m column, Shinwa Chemical Industries). Helium gas used as a carrier gas for the GC analyses. ¹H NMR spectra were measured in CDCl₃ using a JEOL RESONANCE ECA 500 (¹H: 500 MHz) spectrometer. The chemical shifts for ¹H NMR spectra are given in δ (ppm) relative to internal tetramethylsilane. Electrochemical measurements were performed using an electrochemical analyzer (CH Instruments 660C, ALS). Constant current electrolysis experiments were performed using HOKUTO DENKO HABF501A Potentiostat/Galvanostat. Droplet sizes and their distribution were determined by dynamic light scattering (DLS) method at 25 °C with a light scattering photometer (Zetasizer Nano ZS ZEN3600, Sysmex Co.). Before measurement, the samples were diluted to proper concentration. The minimum measurement time of 30 s was required for setup and stabilization of the sample before the first data point was obtained.

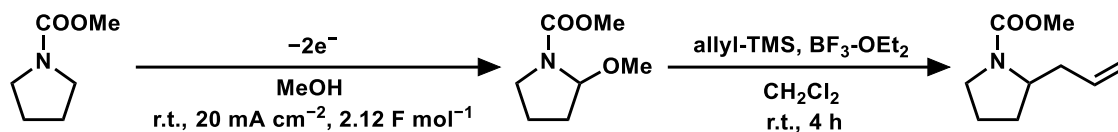
2. Synthesis

N-(Methoxycarbonyl) pyrrolidine (**1**)



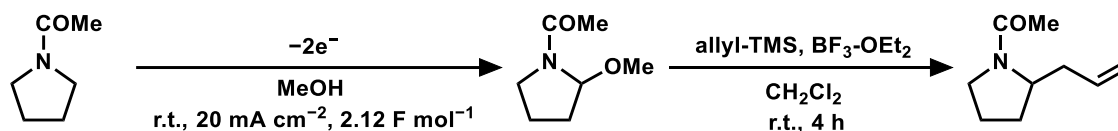
A three necked flask was charged with CH₂Cl₂ (80 mL), Na₂CO₃ (40 g, 0.378 mol) and pyrrolidine (13.6 g, 16.5 mL, 0.20 mol). The solution was refluxed in an oil bath set to 40°C, and methyl chloroformate (20.6 g, 0.22 mol) was added over 2 h at a rate that sustains a gentle reflux. After the addition of methyl chloroformate was completed, the reaction mixture was stirred overnight at room temperature. The mixture was filtered with suction through a filter paper and the filtrate was washed with water (3 × 15 mL). The CH₂Cl₂ layer was dried over Na₂SO₄ and the filtrate after removal of Na₂SO₄ was evaporated. The obtained crude product was purified by silica gel column chromatography (hexane/ethyl acetate = 5/1) to give yellow oil of **1** (78% yield). ¹H NMR spectrum of the product corresponded to the reported data (Fig. S24).⁴

2-Allyl-*N*-(methoxycarbonyl) pyrrolidine (**2**)



Bulk electrolysis was carried out in an undivided cell equipped with a working electrode (graphite plate, 2 cm × 3 cm), and a counter electrode (Pt mesh, ϕ 0.12 mm, 2 cm × 3 cm, 55 mesh) in methanol (40 mL) containing *N*-(methoxycarbonyl) pyrrolidine **1** (2.59 g, 2.35 mL, 20 mmol), tetraethylammonium *p*-toluenesulfonate (1.206 g, 4.0 mmol). Constant current (20 mA cm⁻²) was applied for the electrolysis. After 2.12 F mol⁻¹ of charge was passed, the solvent was removed under reduced pressure. The residue was dissolved in CH₂Cl₂ (30 mL) and washed with brine (15 mL). The aqueous phase was further extracted with CH₂Cl₂ (3 × 15 mL). The combined CH₂Cl₂ phase was dried over MgSO₄ and the filtrate after removal of MgSO₄ was evaporated to get 2-methoxy-*N*-(methoxycarbonyl) pyrrolidine (81% yield). A solution of 2-methoxy-*N*-(methoxycarbonyl) pyrrolidine (1.60 g, 1.43 mL, 10 mmol) and allyltrimethylsilane (8.0 mL, 50 mmol) in dry CH₂Cl₂ (50 mL) was cooled to 0°C under N₂ atmosphere. Then BF₃-OEt₂ (2.5 mL, 20 mmol) was added dropwise. The reaction mixture was allowed to reach room temperature and was stirred for 4 h before being poured into aqueous NaHCO₃ and extracted with CH₂Cl₂. The CH₂Cl₂ phase was dried over Na₂SO₄ and the filtrate after removal of Na₂SO₄ was evaporated. Crude product was purified by silica gel column chromatography (hexane/ethyl acetate = 5/1) to give yellow oil of **2** (66% yield). ¹H NMR spectrum of the product corresponded to the reported data (Fig. S25).⁵

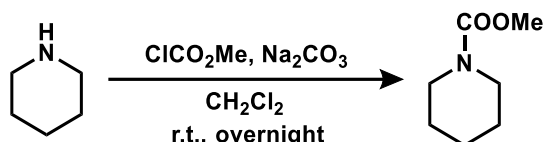
2-Allyl-*N*-acetylpyrrolidine (**4**)



Bulk electrolysis was carried out using undivided cell equipped with a working electrode (graphite plate, 2 cm × 3 cm), and a counter electrode (Pt mesh, ϕ 0.12 mm, 2 cm × 3 cm, 55 mesh) in methanol (40 mL) containing *N*-acetylpyrrolidine **3** (2.26 g, 2.22 mL, 20 mmol), tetraethylammonium *p*-toluenesulfonate (1.206 g, 4.0 mmol). Constant current (20 mA cm⁻²) was applied for the electrolysis. After 2.12 F mol⁻¹ of charge was passed, the solvent was removed under the reduced pressure. The residue was dissolved in CH₂Cl₂ (30 mL) and washed with brine (15 mL). The aqueous phase was further extracted with CH₂Cl₂ (3 × 15 mL). The combined CH₂Cl₂ phase was dried over MgSO₄ and the filtrate after removal of MgSO₄ was evaporated to get 2-methoxy-*N*-acetylpyrrolidine (75% yield). A solution of 2-methoxy-*N*-acetylpyrrolidine (1.43 g, 1.38 mL, 10 mmol) and allyltrimethylsilane (8.0 mL, 50 mmol) in dry CH₂Cl₂ (50 mL) was cooled to 0°C under N₂ atmosphere. Then BF₃-OEt₂ (2.5 mL, 20 mmol) was added dropwise. The reaction mixture was allowed to reach room temperature and

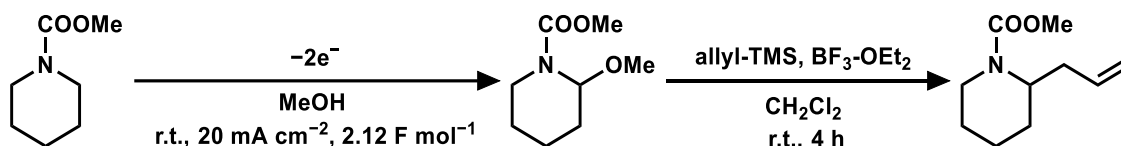
was stirred for 4 h before being poured into aqueous NaHCO₃ and extracted with CH₂Cl₂. The CH₂Cl₂ phase was dried over Na₂SO₄ and the filtrate after removal of Na₂SO₄ was evaporated. Crude product was purified by silica gel column chromatography (hexane/ethyl acetate = 9/1) to give yellow oil of **4** (66% yield). ¹H NMR spectrum of the product corresponded to the reported data (Fig. S26).⁵

N-(Methoxycarbonyl) piperidine (**5**)



A three necked flask was charged with CH₂Cl₂ (80 mL), Na₂CO₃ (40 g, 0.378 mol), and piperidine (17.0 g, 19.7 mL, 0.20 mol). The solution was refluxed in an oil bath set at 40°C, and methyl chloroformate (20.6 g, 0.22 mol) was added over 2 h at a rate that sustains a gentle reflux. After the addition of methyl chloroformate was completed, the reaction mixture was stirred overnight at room temperature. The mixture was filtered with suction through a filter paper and the filtrate was washed with water (3 × 15 mL). The CH₂Cl₂ layer was dried over Na₂SO₄ and the filtrate after removal of Na₂SO₄ was evaporated. The obtained crude product was purified by silica gel column chromatography (hexane/ethyl acetate = 5/1) to give yellow oil of **5** (83% yield). ¹H NMR spectrum of the product corresponded to the reported data (Fig. S27).⁶

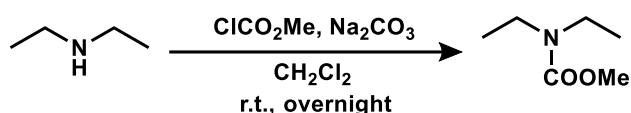
2-Allyl-*N*-(methoxycarbonyl) piperidine (**6**)



Bulk electrolysis was carried out using undivided cell equipped with a working electrode (graphite plate, 2 cm × 3 cm), and a counter electrode (Pt mesh, ϕ 0.12 mm, 2 cm × 3 cm, 55 mesh) in methanol (40 mL) containing *N*-(methoxycarbonyl) piperidine (2.86 g, 2.72 mL, 20 mmol), tetraethylammonium *p*-toluenesulfonate (1.206 g, 4.0 mmol). Constant current (20 mA cm⁻²) was applied for the electrolysis. After 2.12 F mol⁻¹ of charge was passed, the solvent was removed under the reduced pressure. The residue was dissolved in CH₂Cl₂ (30 mL) and washed with brine (15 mL). The aqueous phase was further extracted with CH₂Cl₂ (3 × 15 mL). The combined CH₂Cl₂ phase was dried over MgSO₄ and the filtrate after removal of MgSO₄ was evaporated to get 2-methoxy-*N*-(methoxycarbonyl) piperidine (77% yield). A solution of 2-methoxy-*N*-(methoxycarbonyl) piperidine (1.73 g, 1.61 mL, 10 mmol) and allyltrimethylsilane (8.0 mL, 50 mmol) in dry CH₂Cl₂ (50 mL) was cooled to 0°C under N₂ atmosphere. Then BF₃-OEt₂ (2.5 mL, 20 mmol) was added dropwise. The

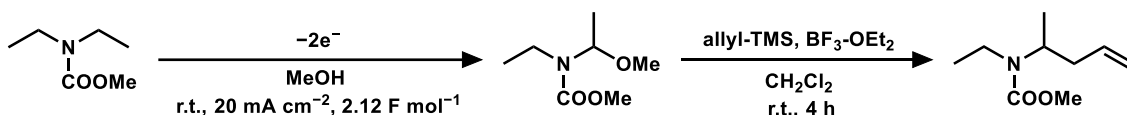
reaction mixture was allowed to reach room temperature and was stirred for 4 h before being poured into aqueous NaHCO₃ and extracted with CH₂Cl₂. The CH₂Cl₂ phase was dried over Na₂SO₄ and the filtrate after removal of Na₂SO₄ was evaporated. Crude product was purified by silica gel column chromatography (hexane/ethyl acetate = 5/1) to give yellow oil of **6** (79% yield). ¹H NMR spectrum of the product corresponded to the reported data (Fig. S28).⁷

Diethyl-carbamic acid methyl ester (7)



A three necked flask was charged with CH₂Cl₂ (80 mL), Na₂CO₃ (40 g, 0.378 mol) and diethylamine (14.6 g, 20.7 mL, 0.20 mol). The solution was refluxed in an oil bath set at 40°C, methyl chloroformate (20.6 g, 0.22 mol) was added over 2 h at a rate that sustains a gentle reflux. After the addition of methyl chloroformate was completed, the reaction mixture was stirred overnight at room temperature. The mixture was filtered with suction through a filter paper and the filtrate was washed with water (3 × 15 mL). The solvent was dried over Na₂SO₄ and the filtrate after removal of Na₂SO₄ was evaporated. Crude product was purified by silica gel column chromatography (hexane/ethyl acetate = 9/1) to give yellow oil of **7** (82% yield). ¹H NMR spectrum of the product corresponded to the reported data (Fig. S29).⁶

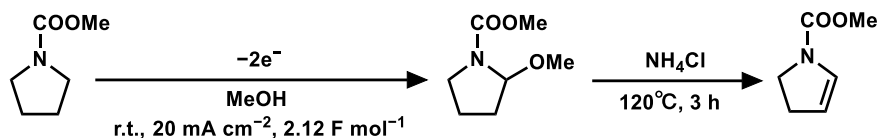
Ethyl-(1-methyl-but-3-enyl)-carbamic acid methyl ester (8)



Bulk electrolysis was carried out using undivided cell equipped with a working electrode (graphite plate, 2 cm × 3 cm), and a counter electrode (Pt mesh, ϕ 0.12 mm, 2 cm × 3 cm, 55 mesh) in methanol (40 mL) containing diethyl-carbamic acid methyl ester **7** (2.62 g, 2.65 mL, 20 mmol), tetraethylammonium *p*-toluenesulfonate (1.206 g, 4.0 mmol). Constant current (20 mA cm⁻²) was applied for the electrolysis. After 2.12 F mol⁻¹ of charge was passed, the solvent was removed under the reduced pressure. The residue was dissolved in CH₂Cl₂ (30 mL), and washed with brine (15 mL). The aqueous phase was further extracted with CH₂Cl₂ (3 × 15 mL). The combined CH₂Cl₂ phase was dried over MgSO₄ and the filtrate after removal of MgSO₄ was evaporated to get ethyl-(1-methoxyethyl)-carbamic acid methyl ester (63% yield). A solution of ethyl-(1-methoxyethyl)-carbamic acid methyl ester (1.61 g, 1.63 mL, 10 mmol) and allyltrimethylsilane (8.0 mL, 50 mmol) in dry CH₂Cl₂ (50 mL) was cooled to 0°C under N₂ atmosphere. Then BF₃-OEt₂ (2.5 mL, 20 mmol) was added dropwise. The reaction mixture was allowed to reach room temperature and was stirred for 4 h

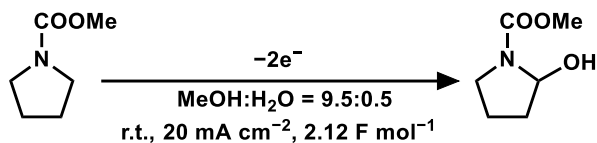
before being poured into aqueous NaHCO₃ and extracted with CH₂Cl₂. The CH₂Cl₂ phase was dried over Na₂SO₄ and the filtrate after removal of Na₂SO₄ was evaporated. Crude product was purified by silica gel column chromatography (hexane/ethyl acetate = 5/2) to give yellow oil of **8** (42% yield). ¹H NMR spectrum of the product corresponded to the reported data (Fig. S30).⁷

N-(methoxycarbonyl)-2-pyrroline



Bulk electrolysis was carried out using undivided cell equipped with a working electrode (graphite plate, 2 cm × 3 cm), and a counter electrode (Pt mesh, ϕ 0.12 mm, 2 cm × 3 cm, 55 mesh) in methanol (40 mL) containing *N*-(methoxycarbonyl) pyrrolidine **1** (2.59 g, 2.35 mL, 20 mmol), tetraethylammonium *p*-toluenesulfonate (1.206 g, 4.0 mmol). Constant current (20 mA cm⁻²) was applied for the electrolysis. After 2.12 F mol⁻¹ of charge was passed, the solvent was removed under the reduced pressure. The residue was dissolved in CH₂Cl₂ (30 mL), and washed with brine (15 mL). The aqueous phase was further extracted with CH₂Cl₂ (3 × 15 mL). The combined CH₂Cl₂ phase was dried over MgSO₄ and the filtrate after removal of MgSO₄ was evaporated to get 2-methoxy-*N*-(methoxycarbonyl) pyrrolidine (81% yield). A solution of 2-methoxy-*N*-(methoxycarbonyl) pyrrolidine (2.70 g, 17 mmol) and ammonium chloride (0.16 g, 2.8 mmol) was heated in an oil bath set to 110 °C and stirred 3 h. The mixture was filtered with suction through a filter paper and evaporated. Crude product was purified by silica gel column chromatography (hexane/ethyl acetate = 1/1) to give yellow oil of *N*-(methoxycarbonyl)-2-pyrroline (25% yield). ¹H NMR spectrum of the product corresponded to the reported data (Fig. S31).³

2-Hydroxy-*N*-(methoxycarbonyl) pyrrolidine



Bulk electrolysis was carried out using undivided cell equipped with a working electrode (graphite plate, 2 cm × 3 cm), and a counter electrode (Pt mesh, ϕ 0.12 mm, 2 cm × 3 cm, 55 mesh) in methanol/water=9.5/0.5 (40 mL) containing *N*-(methoxycarbonyl) pyrrolidine **1** (2.59 g, 2.35 mL, 20 mmol), tetraethylammonium *p*-toluenesulfonate (1.206 g, 4.0 mmol). Constant current (20 mA cm⁻²) was applied for the electrolysis. After 2.12 F mol⁻¹ charge was passed, the solvent was removed under reduced pressure. The residue was dissolved in CH₂Cl₂ (30 mL), and washed with brine (15 mL). The aqueous phase was further extracted with CH₂Cl₂ (3 × 15 mL). The combined CH₂Cl₂ phase was dried over MgSO₄ and the filtrate after removal of MgSO₄ was evaporated. The obtained crude product was

purified by silica gel column chromatography (hexane/ethyl acetate = 2/3) to give yellow oil of 2-Hydroxy-N-(methoxycarbonyl) pyrrolidine (19% yield). ^1H NMR spectrum of the product corresponded to the reported data (Fig. S32).⁸

3. Preparation of emulsion solutions

Various amounts of nucleophile were added to solution of 4.4 mmol substrate in 15 mL of [EMIM][BF₄] to form a biphasic mixture, and the prepared mixture was poured into a Rosette Cooling Cell (Branson Ultrasonics Co.). Sonication was conducted with 20 kHz ultrasound using an ultrasonic stepped horn (3.2 mm diameter, titanium alloy, Branson Ultrasonics Co.) connected with a 20 kHz ultrasound generator (150 W cm⁻², SONIFIER250-D, Branson Ultrasonics Co.). The sequential ultrasonication at 20 kHz followed by 1.6 MHz was carried out using an ultrasonic transducer (16 W cm⁻², Honda Electronics Co. Ltd.) attached to a Pyrex glass cylindrical tube (diameter, 24mm; length, 75mm). Subsequently, the sequential ultrasonication at 20 kHz followed by 1.6 MHz and 2.4 MHz was carried out using an ultrasonic transducer (8 W cm⁻², Honda Electronics Co. Ltd.) attached to a Pyrex glass cylindrical tube (diameter, 24mm; length, 75mm).

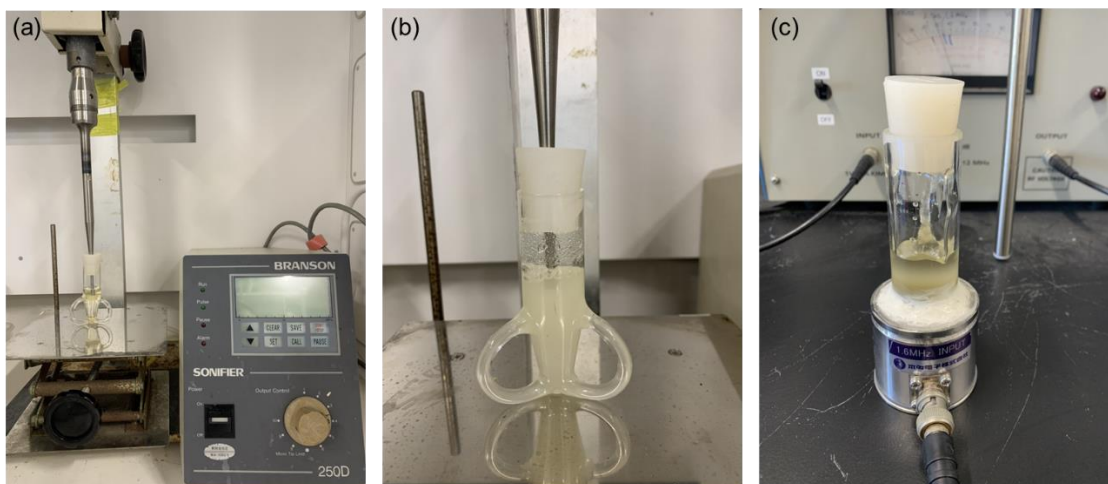


Fig. S1 Photograph of sonication instruments. (a) Ultrasonic stepped horn and 20 kHz ultrasound generator. (b) Sonication at 20 kHz frequency. (c) Sonication at 1.6 MHz frequency.

4. Fabrication of a flow microreactor

Fig. S2 shows fabrication procedure for an electrochemical flow microreactor. The reactor was fabricated with glass plates and two platinum (Pt) plates (3 cm width, 3 cm length each). A spacer (with thickness adjusted by laminating 20 μm thick and 80 μm thick double faced adhesive tapes together) used to leave a rectangular channel exposed, and the two electrodes were simply sandwiched together. The area of the two electrodes were 1.33 cm \times 3 cm. After connecting Teflon tube (inner diameter, 0.8 mm; outer diameter, 1.4 mm; #9003; Nichias) to inlet and outlet, the reactor was sealed with epoxy resin (Araldite AR-R30, Nichiban).

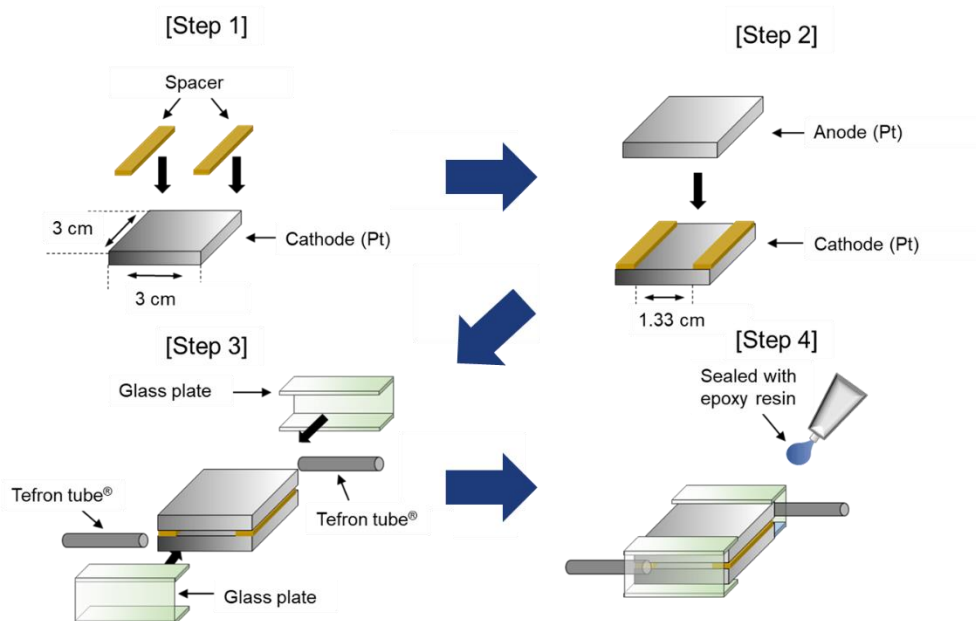


Fig. S2 Fabrication procedure for the electrochemical flow microreactor.

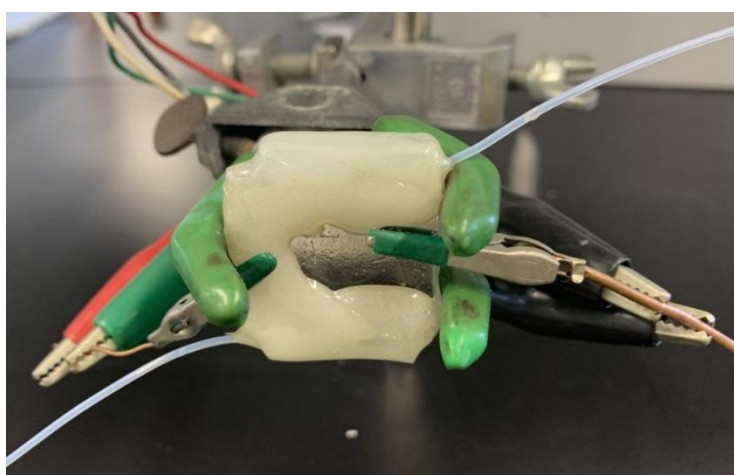


Fig. S3 Photograph of the electrochemical flow microreactor.

5. Linear sweep voltammetry

Linear sweep voltammetry (LSV) measurements were performed in a beaker type cell using a bi-potentiostat (ALS2323). A platinum disk (3.0 mm diameter, BAS) and platinum plate (2 cm × 2 cm, Nilaco) were used as a working electrode and a counter electrode, respectively. An Ag wire (0.70 mm diameter, Nilaco) was used as a quasi-reference electrode. Ferrocene/ferrocenium redox couple (Fc/Fc⁺) was used as an internal reference for all electrochemical studies, and the potentials are reported with respect to the formal potential of Fc/Fc⁺ redox couple.

6. General procedure for electrolysis in the two-phase emulsion system using the flow microreactor

Unless otherwise stated, a two-phase emulsion solution was prepared by sequential ultrasonication at 20 kHz followed by 1.6 MHz. The prepared emulsion solution was introduced into the electrochemical flow microreactor using a syringe pump (KDS-100, kdScientific) under flow rate control. Then, constant current was applied for electrolysis. After the electrolysis, a reaction mixture was extracted with toluene and subjected to GC to determine the current efficiency (Fig. S13-S23). Electricity was calculated according to the following equation.

$$\text{Electricity [F mol}^{-1}\text{]} = \frac{\text{Charge passed in microreactor per second [F s}^{-1}\text{]}}{\text{Substrate introduced into microreactor per second [mol s}^{-1}\text{]}}$$

$$= \frac{\frac{1}{96485} [\text{F C}^{-1}] \times \left(\text{Current density [mA cm}^{-2}\text{]} \times \frac{1}{1000} [\text{A mA}^{-1}\text{]} \times \text{Electrode surface area [cm}^2\text{]} \right) [\text{C s}^{-1}\text{]}}{\left(\text{flow rate [mL h}^{-1}\text{]} \times \frac{1}{1000} [\text{L mL}^{-1}\text{]} \times \frac{1}{3600} [\text{h s}^{-1}\text{]} \times \text{Concentration of substrate [mol L}^{-1}\text{]} \right) [\text{mol s}^{-1}\text{]}}$$

$$\text{Current efficiency [\%]} = \frac{\text{Experimentally obtained amount of a product after passing a specific charge [mol]}}{\text{Theoretical amount of a product after passing a specific charge [mol]}}$$

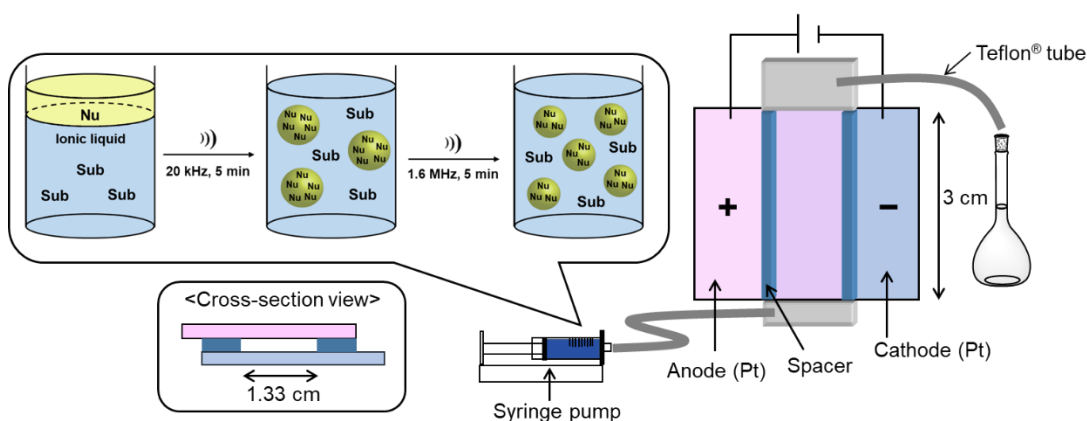


Fig. S4 Scheme of the anodic substitution reaction in the acoustic emulsified solution by using the flow microreactor.

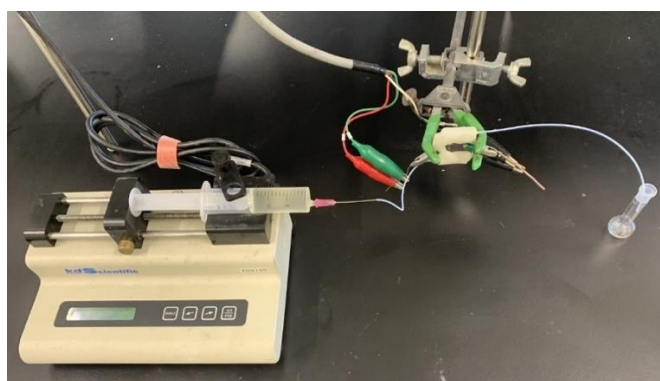


Fig. S5 Photograph of the electrochemical flow microreactor and a syringe pump.

7. Procedure for electrolysis in the one-phase system using the flow microreactor

A 15 mL of 0.1 M $\text{Bu}_4\text{NBF}_4/\text{MeCN}$ solution containing 4.4 mmol of substrate **1** and 3.6 mmol of allyl-TES was introduced into the electrochemical flow microreactor using a syringe pump (KDS-100, kdScientific) under flow rate control (15 mL h^{-1}). Then, constant current (23.4 mA cm^{-2}) was applied for electrolysis. After the charge passed (0.2 F mol^{-1} of **1**), a reaction mixture was subjected to GC to determine the current efficiency (Fig. S13, S17, S18).

8. Procedure for electrolysis in the two-phase emulsion system using the batch type reactor

A two-phase emulsion solution consisting of 15 mL of $[\text{EMIM}][\text{BF}_4]$ with soluble substrate **1** (4.4 mmol) and insoluble allyl-TES (3.6 mmol) was prepared by sequential ultrasonication at 20 kHz followed by 1.6 MHz. The irradiation time at each frequency was 5 min. This solution was added to the undivided cell equipped with a working electrode (Pt plate, $2 \text{ cm} \times 2 \text{ cm}$, Nilaco) and a counter electrode (Pt plate, $2 \text{ cm} \times 2 \text{ cm}$, Nilaco). The distance between two electrodes was set to *ca.* 1 cm. Then, constant current (23.4 mA cm^{-2}) was applied for electrolysis. After the charge passed (0.2 F mol^{-1} of **1**), a reaction mixture was extracted with toluene and subjected to GC to determine the current efficiency (Fig. S13, S17, S18). Photograph of a batch type reactor is shown in Fig. S6.

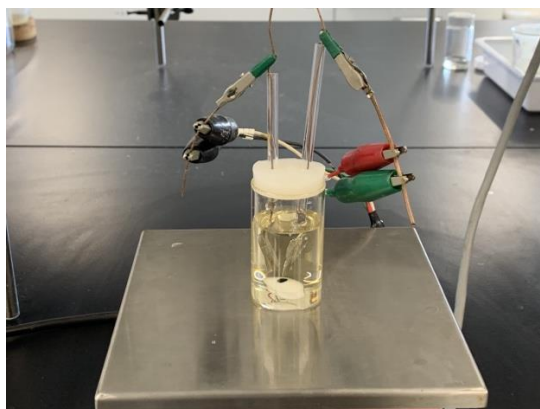


Fig. S6. Photograph of batch type reactor

9. Linear sweep voltammograms for the oxidation of substrate **1**, allyl-TES, and product **2** in the one-phase system

A 15 mL of 0.1 M Bu₄NBF₄/MeCN solution containing 0.3 mmol of substrate **1**, 0.3 mmol of allyl-TES, or 0.3 mmol of product **2** was added to a beaker type cell for LSV measurements. N₂ gas was sparged through the electrolyte solution with stirring for at least 30 min. Voltammograms were recorded using a platinum disk electrode (3.0 mm diameter), and a platinum plate electrode (2 cm × 2 cm) as a working electrode and a counter electrode, respectively, at a scan rate of 0.1 V s⁻¹.

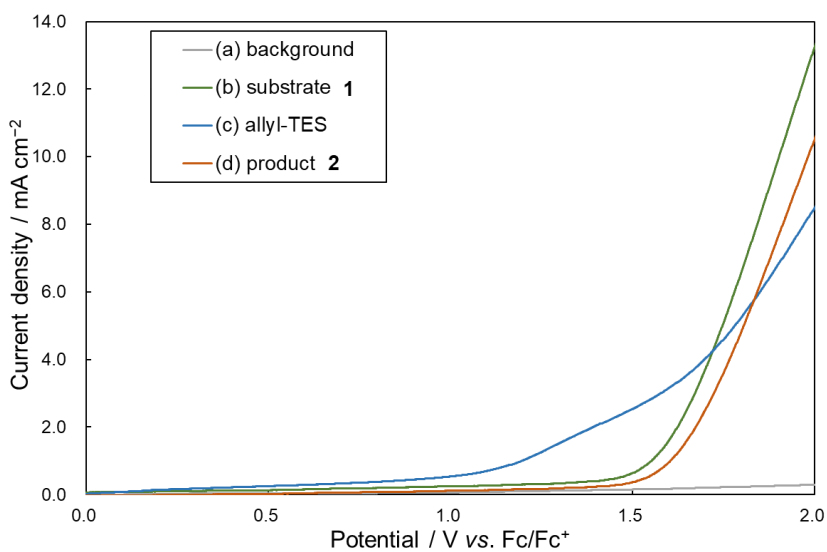
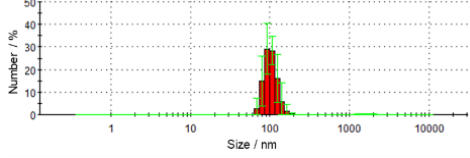
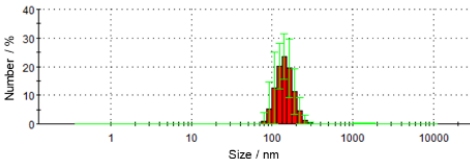
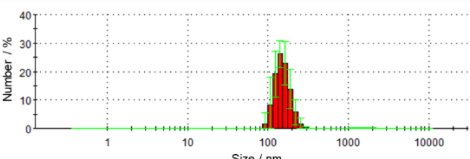


Fig. S7 Linear sweep voltammograms of (a) background, (b) 20 mM substrate **1**, (c) 20 mM allyl-TES, and (d) 20 mM product **3** in 0.1 M Bu₄NBF₄/MeCN.

10. Stability of an allyl-TES emulsion solution prepared by tandem acoustic emulsification

An allyl-TES emulsion solution was prepared according to the procedure described above (see 3. Preparation of emulsion solution). Subsequently, the prepared emulsion was subjected to DLS measurements immediately after emulsification, after 1 hour, and after passing through the reactor.

Table S1. Time-dependent change of the size distribution and the average diameter of the nucleophile emulsion droplets formed by two-step ultrasonication (20 kHz→1.6 MHz)^a

	Size distribution	Average diameter / nm
Immediately after emulsification		132
After 1 hour		156
After passing through the electrochemical flow microreactor		218

^aExperimental conditions: continuous phase, solution of 4.4 mmol substrate **1** in 15 mL of [EMIM][BF₄]; dispersed phase, 3.6 mmol of allyl-TES. Emulsification condition: 20 kHz (5 min) →1.6 MHz (5 min).

11. Electrolysis in the two-phase emulsion system using the flow microreactor at various experimental parameters

To determine the optimum conditions, the anodic substitution reaction was carried out in the allyl-TES emulsion solution using the flow microreactor at various experimental parameters (amount of nucleophile, electrode distance, flow rate, and current density) that are expected to affect the electrolysis (Fig. S8).

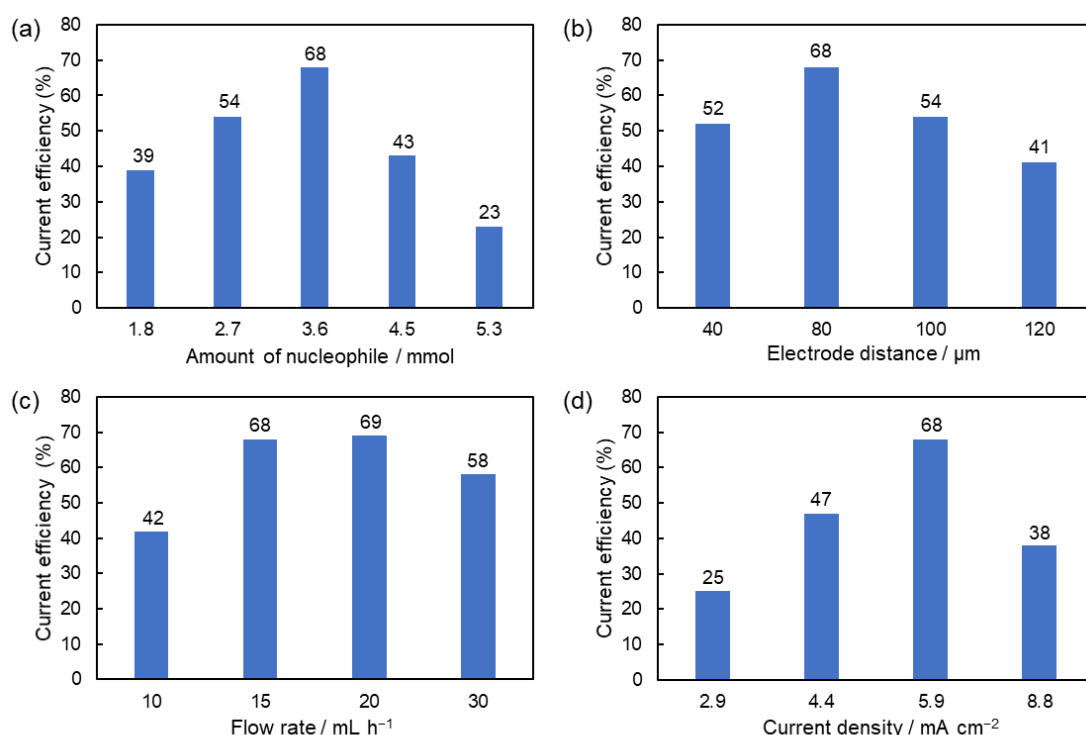


Fig. S8 Effect of the (a) amount of nucleophile, (b) electrode distance, (c) flow rate, and (d) current density on the current efficiency. Emulsification condition: 20 kHz (5 min) \rightarrow 1.6 MHz (5 min).

The current efficiency increased with increasing the amount of nucleophile at ranging from 1.8 to 3.6 mmol, while it decreased at amounts higher than 4.5 mmol (Fig. S8a). When the amount of allyl-TES is small, the reaction is slow and the unstable iminium cation would have decomposed. On the other hand, as the amount of allyl-TES increased, the elution rate for allyl-TES from the droplets into the [EMIM][BF₄] phase became faster, and the competitive oxidation for allyl-TES in the [EMIM][BF₄] phase became more pronounced.

In order to qualitatively observe elution of allyl-TES into the [EMIM][BF₄] phase, LSV measurements of oxidation in emulsion solutions containing different amounts of nucleophile (1.8, 3.6, and 5.3 mmol) were recorded (Fig. S9). In all cases, faradaic currents derived from the nucleophile

oxidation were observed, indicating allyl-TES was partially dissolved in the [EMIM][BF₄] phase. Also, as expected, its current value was larger when the amount of nucleophile was 5.3 mmol. Given that the saturation concentration of allyl-TES in [EMIM][BF₄] is constant, it was suggested that the elution rate for allyl-TES from the droplet to compensate for the consumption of oxidized allyl-TES in the [EMIM][BF₄] phase increased with the amount of allyl-TES.

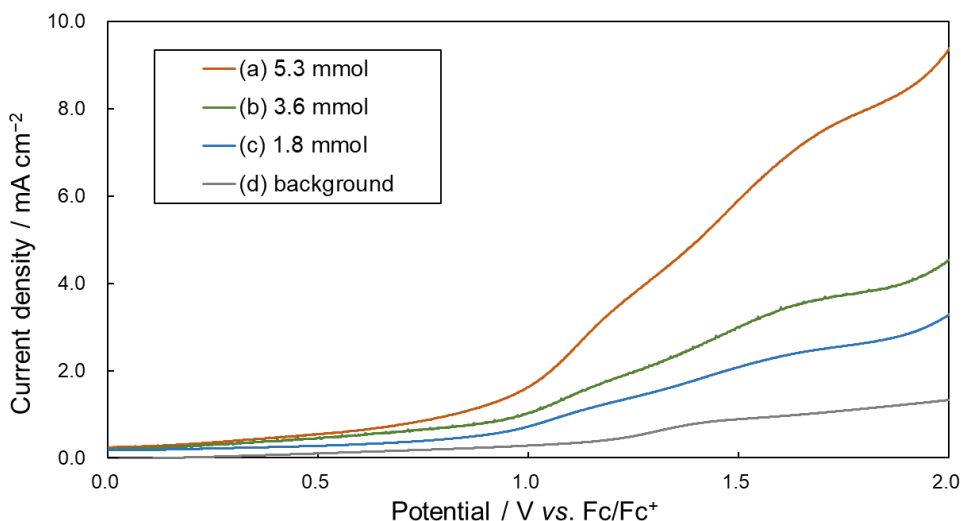


Fig. S9 Linear sweep voltammograms of the two-phase emulsion systems. (a) 5.3 mmol of allyl-TES, (b) 3.6 mmol of allyl-TES, (c) 1.8 mmol of allyl-TES, and (d) background (without allyl-TES) in 15 mL of [EMIM][BF₄]. Emulsification condition was 20 kHz (5 min) → 1.6 MHz (5 min).

Then, the electrode distance of the flow microreactor was then optimized. As shown in Fig. S7b, the current efficiency peaked at the electrode distance of 80 μm . The current efficiency decreased at a narrower distance such as 40 μm , presumably due to the cathodic reduction of iminium cation, which was generated at the anode and diffuse in a short distance to reach the cathode (Fig. S10a). On the other hand, the current efficiency also decreased at distances wider than 100 μm (Fig. S10b). This may be ascribed that the decrease in the surface-to-volume ratio makes it difficult for carbamate to reach the anode during the residence time.

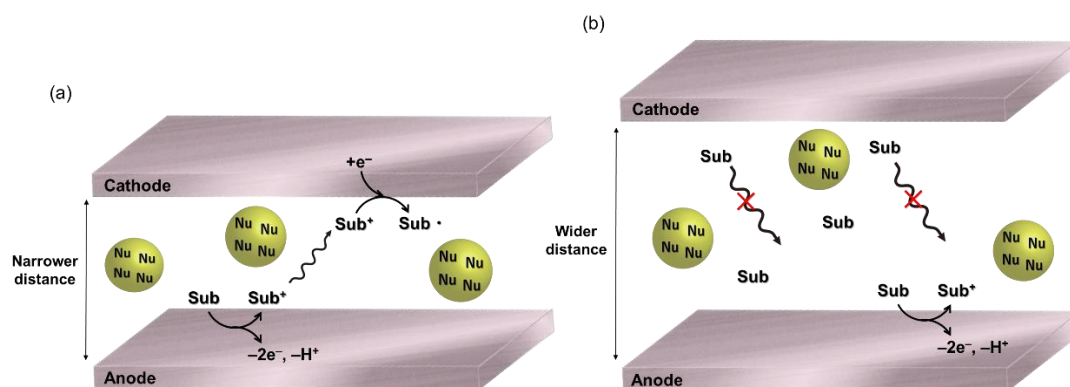


Fig. S10 Schematic image of (a) the cathodic reduction of iminium cation at a narrower electrode distance and (b) the diffusion of carbamate at a wider electrode distance.

To support this discussion, the conversion of carbamate **1** was also measured. A main purpose for this study is not to isolate the reaction products but to clarify the characteristics of a new system for the anodic substitution reaction. Therefore, in the present work, only small amount of electricity was passed to avoid a drastic change in the concentration of carbamate **1** during the electrolysis. For this reason, the conversion never reaches 100%. Therefore, the conversion based on the amount of electricity actually passed during the electrolysis was calculated according to the following equation, and the amount of substrate consumed was compared (Table S2).

Conversion based on the amount of electricity [%]

$$= \text{Conversion} [\%] \times \frac{\text{Theoretical electricity} [\text{F mol}^{-1}]}{\text{Electricity passed during the electrolysis} [\text{F mol}^{-1}]}$$

As shown in Table 2, the conversion based on the amount of electricity decreased at wider distances.

Table S2. Effect of the electrode distance on conversion and current efficiency^a

Entry	Electrode distance / μm	Conversion ^b (%)	Conversion based on the amount of electricity (%)	Current efficiency ^b (%)
1	40	8.0	80	52
2	80	8.3	83	68
3	100	6.8	68	54
4	120	6.1	61	41

^aExperimental conditions: anode, Pt plate (4 cm^2); cathode, Pt plate (4 cm^2); continuous phase, solution of 4.4 mmol substrate **1** in 15 mL of [EMIM][BF₄]; dispersed phase, 3.6 mmol of allyl-TES; flow rate, 15 mL h⁻¹; current density, 5.9 mA cm⁻²; electricity, 0.20 F mol⁻¹. Emulsification condition: 20 kHz (5 min) \rightarrow 1.6 MHz (5 min). ^bDetermined by GC.

As shown in Fig. S8c, the current efficiency was relatively high at flow rates of 15 and 20 mL h⁻¹. At a slower flow rate (10 mL h⁻¹), the current efficiency decreased to 42%, presumably because the longer residence time of product **2** lead to its overoxidation. A higher flow rate (30 mL h⁻¹) also caused the decrease in the current efficiency down to 58%. We attributed this to the shorter residence time, and as a result the conversion of carbamate **1** decreased (Table S3).

Table S3. Effect of the flow rate on conversion and current efficiency^a

Entry	Flow rate / mL h ⁻¹	Electricity / F mol ⁻¹	Conversion ^b (%)	Conversion based on the amount of electricity (%)	Current efficiency ^b (%)
1	10	0.30	12	79	42
2	15	0.20	8.3	83	68
3	20	0.15	6.2	83	69
4	30	0.10	3.0	60	58

^aExperimental conditions: anode, Pt plate (4 cm²); cathode, Pt plate (4 cm²); continuous phase, solution of 4.4 mmol substrate **1** in 15 mL of [EMIM][BF₄]; dispersed phase, 3.6 mmol of allyl-TES; electrode distance, 80 μm; current density, 5.9 mA cm⁻². Emulsification condition: 20 kHz (5 min) → 1.6 MHz (5 min). ^bDetermined by GC.

In the next, effect of current density on efficiency was also investigated. As shown in Fig. S8d, the current efficiency increased with an increase in the current density, and peaked at 5.9 mA cm⁻². The efficiency decreased dramatically at 8.8 mA cm⁻². In this case, the oxidation of [EMIM][BF₄] used as a solvent might occur due to such a high current density condition. In fact, the anodic potential during the electrolysis was found to be much higher than the oxidation potential of [EMIM][BF₄] (2.5 V, Table S4). As a factor for the decrease in current efficiency at lower current densities, it has been pointed out that if the anodic consumption of allyl-TES in the [EMIM][BF₄] phase is slow enough to be compensated by elution from the droplet, most of the anodic current may have been consumed by the oxidation of allyl-TES, which is gradually replenished from the droplet.

Table S4. Effect of the current density on the anode potential and current efficiency^a

Entry	Current density / mA cm ⁻²	Electricity / F mol ⁻¹	Anode potential / V vs. Fc/Fc ⁺	Current efficiency ^b (%)
1	2.9	0.10	1.6	25
2	4.4	0.15	1.7	47
3	5.9	0.20	2.2	68
4	8.8	0.30	2.9	38

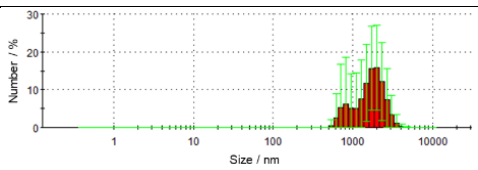
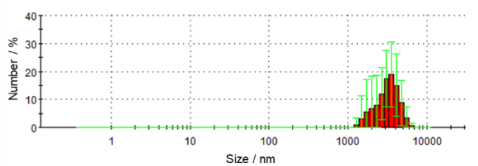
^aExperimental conditions: anode, Pt plate (4 cm²); cathode, Pt plate (4 cm²); continuous phase, solution of 4.4 mmol substrate **1** in 15 mL of [EMIM][BF₄]; dispersed phase, 3.6 mmol of allyl-TES; electrode distance, 80 μm; flow rate, 15 mL h⁻¹. Emulsification condition: 20 kHz (5 min) → 1.6 MHz (5 min).

^bDetermined by GC.

12. Effect of emulsification conditions on the stability of emulsions

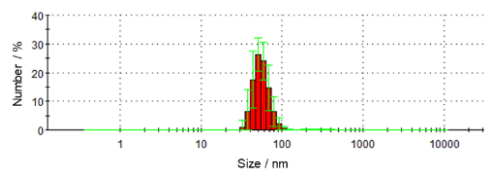
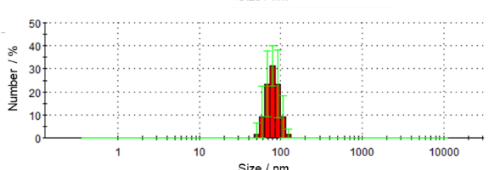
Time-dependent changes of the size distribution and average diameter of the emulsion droplets of allyl-TES formed by 20 kHz ultrasonication (Table S5) and three-step ultrasonication (Table S6) were investigated using DLS measurements.

Table S5. Time-dependent change of the size distribution and average diameter of the emulsion droplets of allyl-TES formed by 20 kHz ultrasonication^a

	Size distribution	Average diameter / nm
Immediately after emulsification		1202
After 1 hour		3372

^aExperimental conditions: continuous phase, solution of 4.4 mmol substrate **1** in 15 mL of [EMIM][BF₄]; dispersed phase, 3.6 mmol of allyl-TES. Emulsification condition: 20 kHz (5 min).

Table S6. Time-dependent change of the size distribution and average diameter of the emulsion droplets of allyl-TES formed by three-step ultrasonication (20 kHz→1.6 MHz→2.4 MHz)^a

	Size distribution	Average diameter / nm
Immediately after emulsification		59
After 1 hour		86

^aExperimental conditions: continuous phase, solution of 4.4 mmol substrate **1** in 15 mL of [EMIM][BF₄]; dispersed phase, 3.6 mmol of allyl-TES. Emulsification condition: 20 kHz (5 min) →1.6 MHz (5 min) →2.4 MHz (5 min).

13. Linear sweep voltammograms of allyl-TES in the two-phase emulsion system prepared by various emulsification conditions

Two-phase emulsion solutions consisting of 15 mL of [EMIM][BF₄] and 3.6 mmol of allyl-TES were prepared by each ultrasonication step in the tandem operation. The emulsion solution was added to a beaker type cell for LSV measurements. Voltammograms were recorded using a platinum disk electrode (3.0 mm diameter), and a platinum plate electrode (2 cm × 2 cm) as a working electrode and a counter electrode, respectively, at a scan rate of 0.1 V s⁻¹.

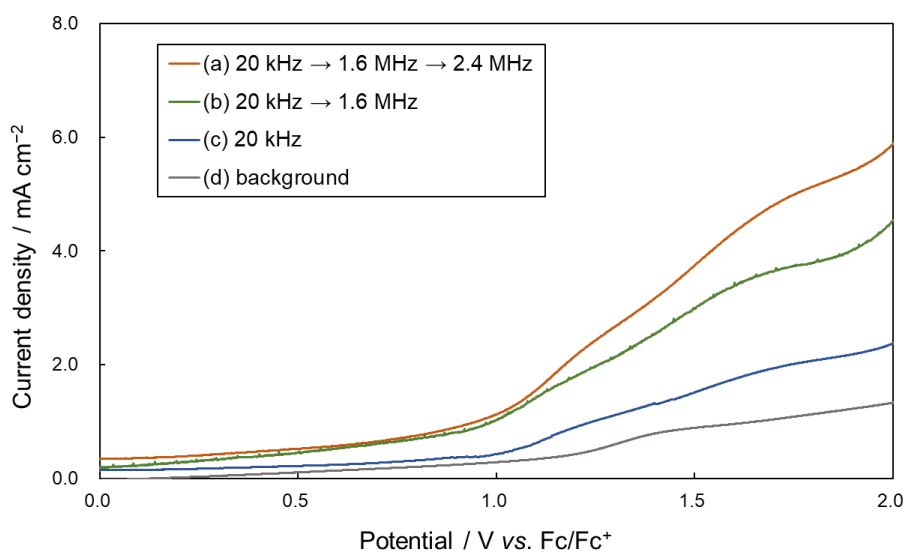


Fig. S11 Linear sweep voltammograms of 3.6 mmol of allyl-TES in the two-phase emulsion system prepared by various emulsification conditions, (a) 20 kHz (5 min) → 1.6 MHz (5 min) → 2.4 MHz (5 min), (b) 20 kHz (5 min) → 1.6 MHz (5 min), (c) 20 kHz (5 min), and (d) without allyl-TES (background).

14. Linear sweep voltammograms of various allyl nucleophiles in the one-phase system

A 15 mL of 0.1 M $\text{Bu}_4\text{NBF}_4/\text{MeCN}$ solution containing 0.3 mmol of allyl-TMS, 0.3 mmol of allyl-TES, or 0.3 mmol of allyl-TIPS was added to a beaker type cell for LSV measurements. N_2 gas was sparged through the electrolyte solution with stirring for at least 30 min. Voltammograms were recorded using a platinum disk electrode (3.0 mm diameter), and a platinum plate electrode ($2\text{ cm} \times 2\text{ cm}$) as a working electrode and a counter electrode, respectively, at a scan rate of 0.1 V s^{-1} .

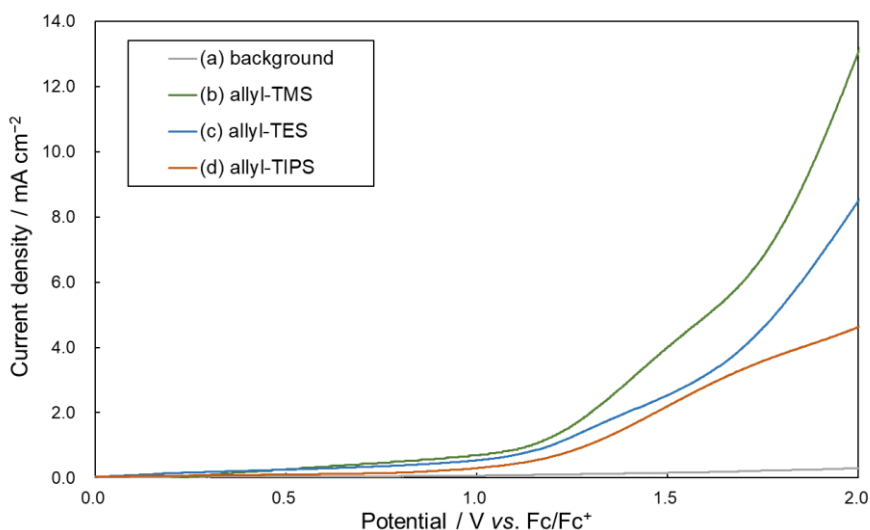


Fig. S12 Linear sweep voltammograms of (a) background (without allyl nucleophiles), (b) 20 mM allyl-TMS, (c) 20 mM allyl-TES, and (d) 20 mM allyl-TIPS in 0.1 M $\text{Bu}_4\text{NBF}_4/\text{MeCN}$.

15. Size distribution and average diameter of emulsion droplets of various allyl nucleophiles

Allyl-TMS, allyl-TES, and allyl-TIPS emulsion solutions were prepared according to the procedure described above (see 3. Preparation of emulsion solution). Subsequently, the prepared emulsion solutions were subjected to DLS measurements immediately after the preparation.

Table S7. Size distribution and average diameter of emulsion droplets of various allyl nucleophiles^a

Entry	Nucleophile	Emulsification condition	Size distribution	Average diameter / nm
1		20 kHz (7 min) → 1.6 MHz (7 min)		145
2		20 kHz (5 min) → 1.6 MHz (5 min)		132
2		20 kHz (10 min) → 1.6 MHz (10 min)		174

^aExperimental conditions: continuous phase, solution of 4.4 mmol substrate **1** in 15 mL of [EMIM][BF₄]; dispersed phase, 3.6 mmol of nucleophile.

16. Linear sweep voltammograms of various allyl nucleophiles in the two-phase emulsion system

Two-phase emulsion solutions consisting of 15 mL of [EMIM][BF₄] and 3.6 mmol of nucleophile (allyl-TMS, allyl-TES, or allyl-TIPS) were prepared by sequential ultrasonication at 20 kHz followed by 1.6 MHz. The emulsion solution was transferred to a beaker type cell for LSV measurements. Voltammograms were recorded using a platinum disk electrode (3.0 mm diameter), and a platinum plate electrode (2 cm × 2 cm) as a working electrode and a counter electrode, respectively, at a scan rate of 0.1 V s⁻¹.

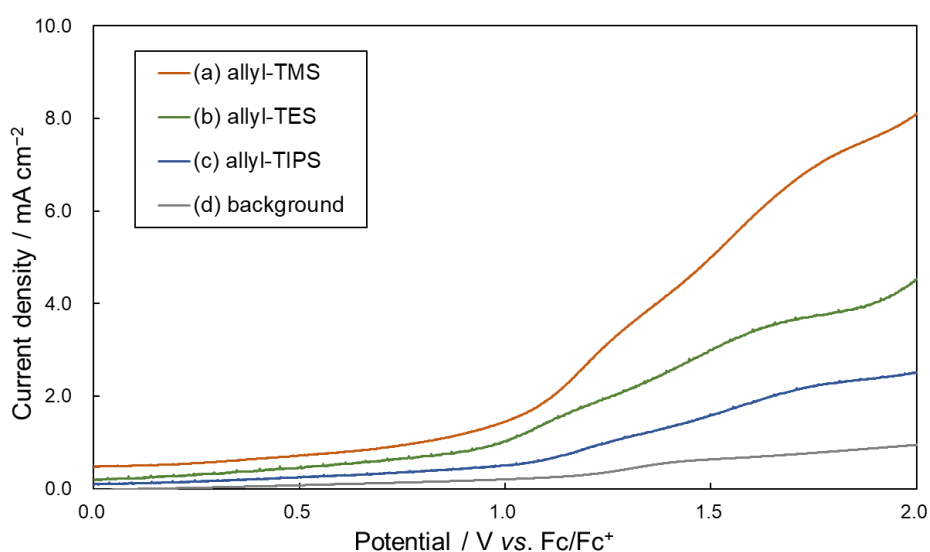
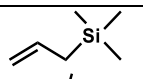
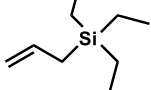
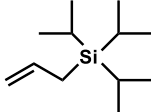


Fig. S13 Linear sweep voltammograms of 3.6 mmol of (a) allyl-TMS, (b) allyl-TES, (c) allyl-TMS, and (d) without nucleophile (background) in the two-phase emulsion system.

17. Effect of the allyl nucleophiles on current efficiency for the detectable products

Table S8 shows the effect of the allyl nucleophile species on current efficiency for the detectable products.

Table S8. Effect of the allyl nucleophiles on current efficiency for the products ^a

Entry	Nucleophile	Current efficiency ^b (%)		
		Allyl-product	β -Proton elimination product	α -Hydroxylated product
1 ^c		34	3.0	3.1
2 ^d		68	4.2	4.0
3 ^e		29	8.4	7.4

^aExperimental conditions: anode, Pt plate (4 cm²); cathode, Pt plate (4 cm²); continuous phase, solution of 4.4 mmol substrate **1** in 15 mL of [EMIM][BF₄]; dispersed phase, 3.6 mmol of nucleophile; electrode distance, 80 μ m; flow rate, 15 mL h⁻¹; current density, 5.9 mA cm⁻²; electricity, 0.2 F mol⁻¹.

^bDetermined by GC. ^cEmulsification condition: 20 kHz (5 min) \rightarrow 1.6 MHz (7 min). ^dEmulsification condition: 20 kHz (5 min) \rightarrow 1.6 MHz (5 min). ^eEmulsification condition: 20 kHz (10 min) \rightarrow 1.6 MHz (10 min).

18. Effect of the presence of various carbamates on the allyl-TES emulsion droplets

Since the state of the allyl-TES emulsion depends on the type of carbamate (substrate), the emulsification conditions were adjusted to keep the average diameter of nucleophile droplets around 100-200 nm (Table S9).

Table S9. Size distribution and average diameter of the allyl-TES emulsion droplets in the presence of various carbamates^a

Entry	Substrate	Emulsification condition	Size distribution	Average diameter / nm
1	 <chem>CN(C)C(=O)OC1CCCN1</chem> 1	20 kHz (5 min) → 1.6 MHz (5 min)		132
2	 <chem>CN(C)C(=O)OC1CCCN1</chem> 3	20 kHz (7 min) → 1.6 MHz (7 min)		135
3	 <chem>CN(C)C(=O)OC1CCNCC1</chem> 5	20 kHz (10 min) → 1.6 MHz (10 min)		144
4	 <chem>CN(C)C(=O)OC1CCN(CC)CC1</chem> 7	20 kHz (5 min) → 1.6 MHz (7 min)		129

^aExperimental conditions: continuous phase, 15 mL of [EMIM][BF₄] dissolved 4.4 mmol of substrate; dispersed phase, 3.6 mmol of allyl-TES.

19. GC analysis

Typical examples of GC charts and calibration curves for GC-FID analysis are shown below.

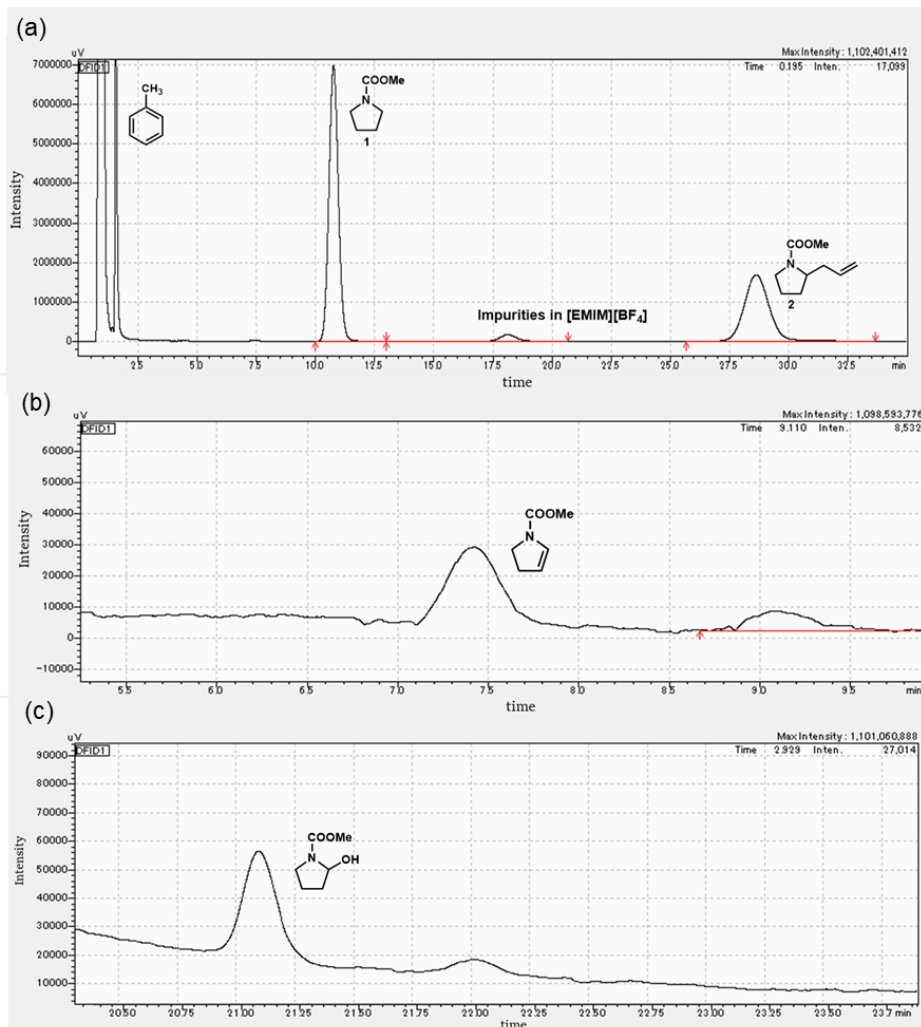


Fig. S14 GC chart of reaction mixture of substrate **1** and allyl-TES after extraction with toluene (corresponding to Entry 1 of Table 3). (a) Overall view, (b) enlarged view of the peak of the β -proton elimination product, (c) enlarged view of the peak of the α -hydroxylated product.

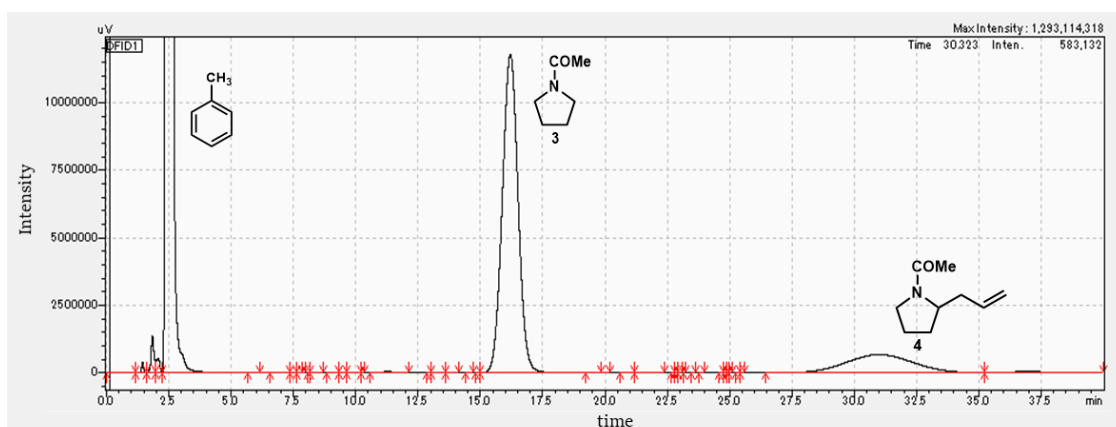


Fig. S15 GC chart of reaction mixture of substrate 3 and allyl-TES after extraction with toluene (corresponding to Entry 2 of Table 3).

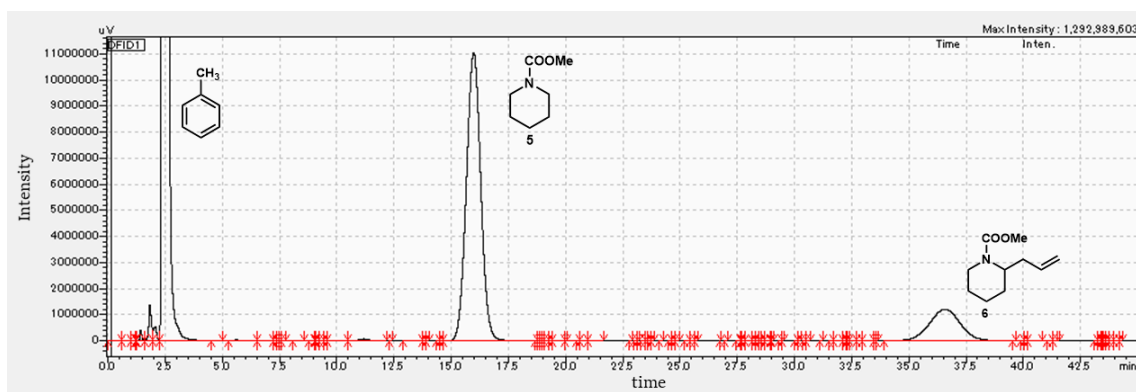


Fig. S16 GC chart of reaction mixture of substrate 5 and allyl-TES after extraction with toluene (corresponding to Entry 3 of Table 3).

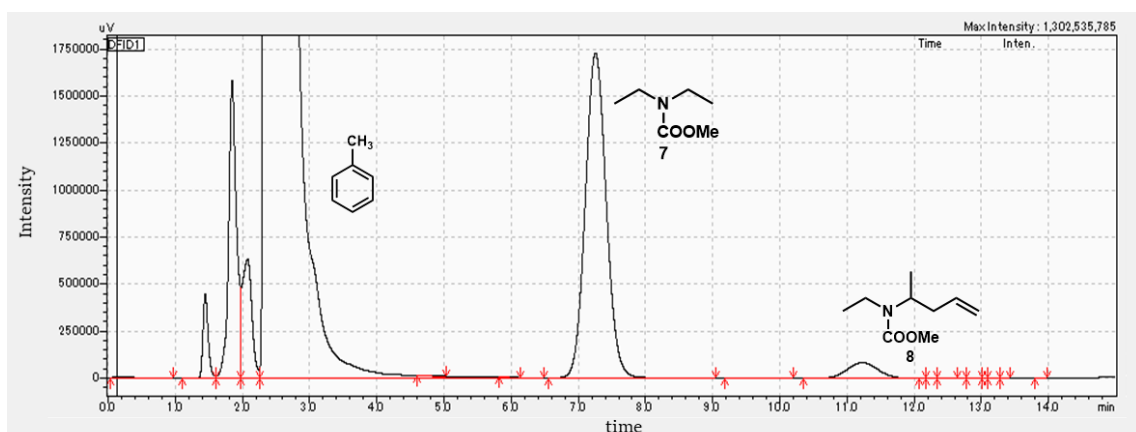


Fig. S17 GC chart of reaction mixture of substrate 7 and allyl-TES after extraction with toluene (corresponding to Entry 4 of Table 3).

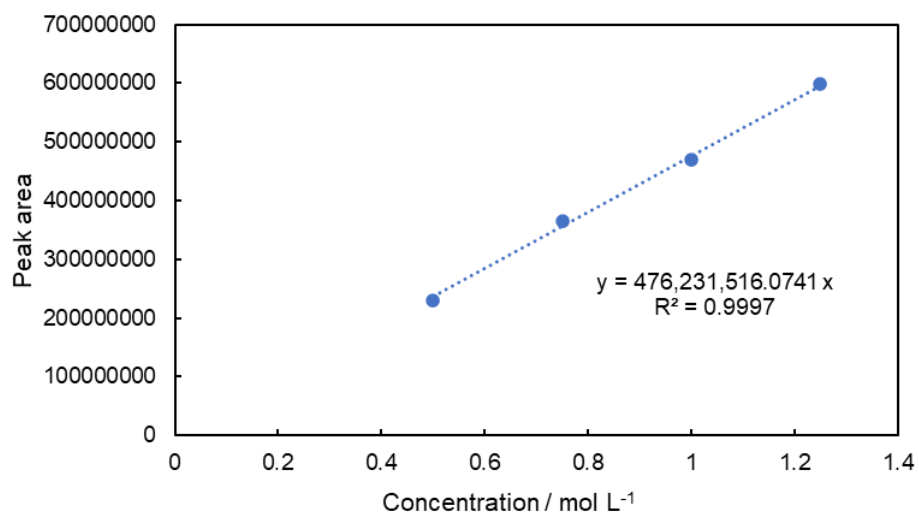


Fig. S18 Calibration curve of carbamate 1 for GC-FID analysis.

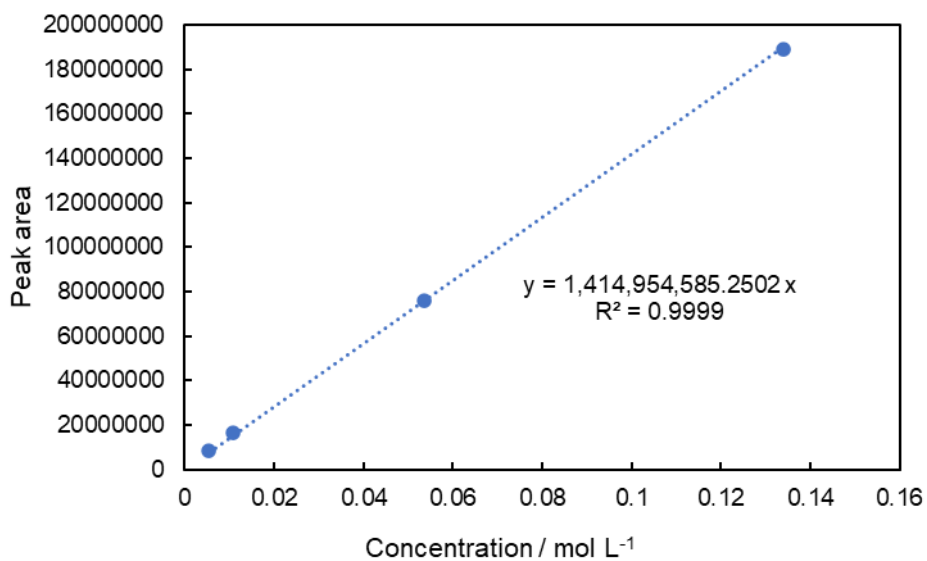


Fig. S19 Calibration curve of product 2 for GC-FID analysis.

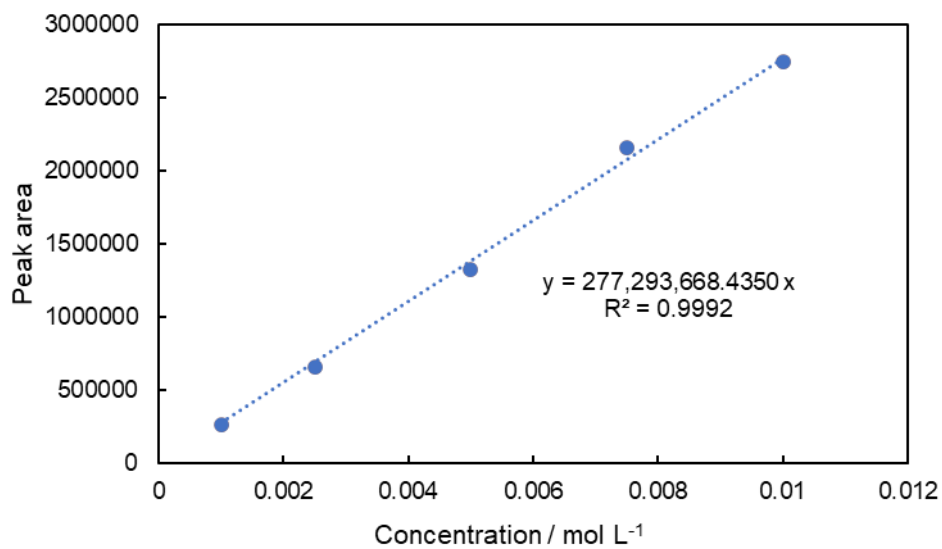


Fig. S20 Calibration curve of β -proton elimination product for GC-FID analysis.

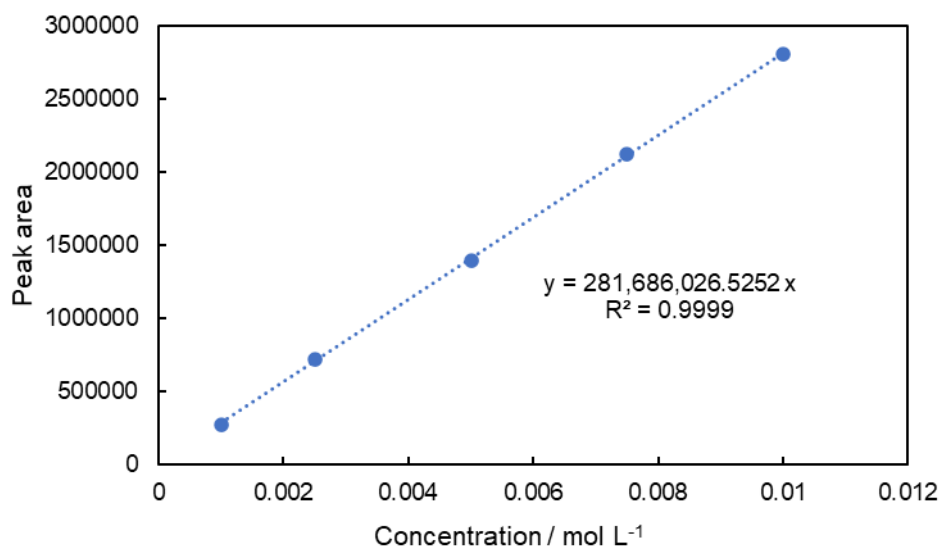


Fig. S21 Calibration curve of α -hydroxylated product for GC-FID analysis.

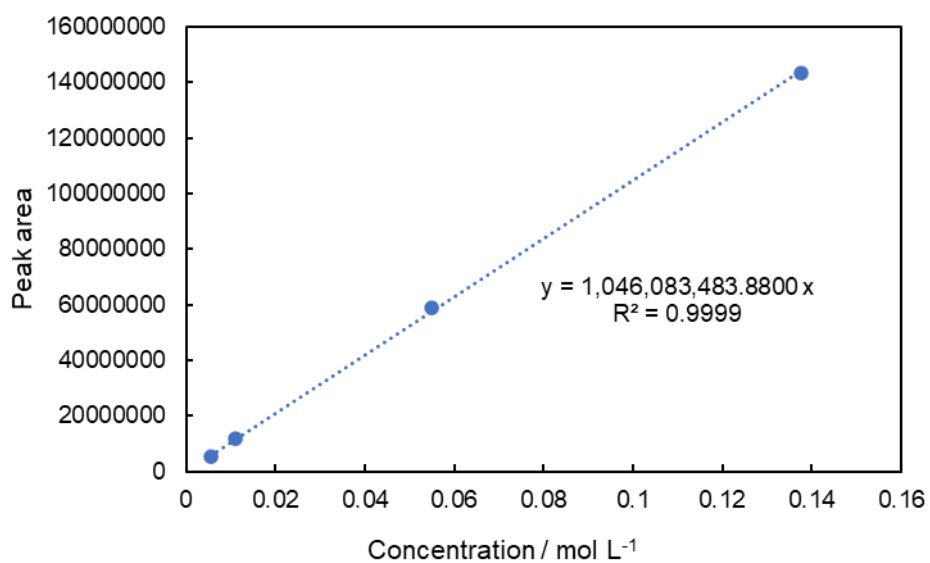


Fig. S22 Calibration curve of product 4 for GC-FID analysis.

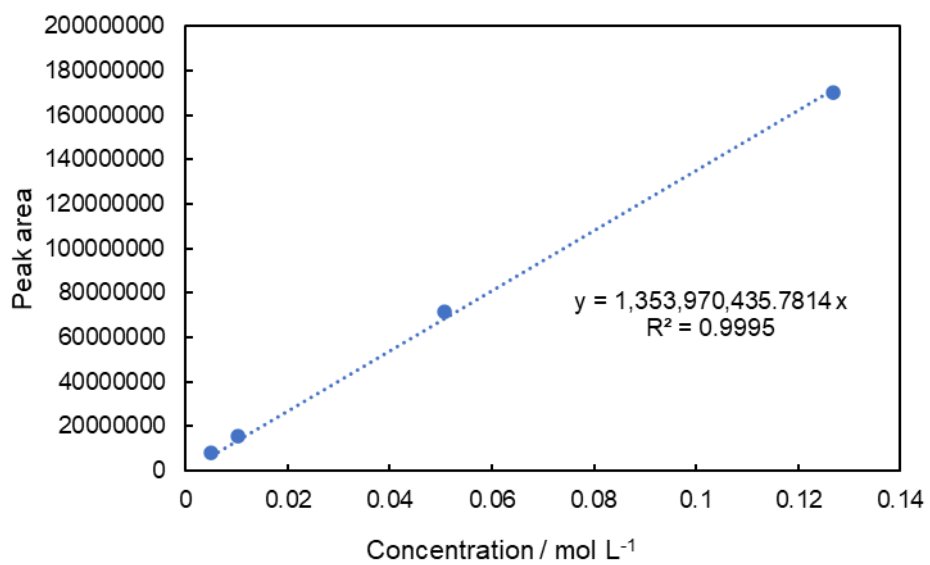


Fig. S23 Calibration curve of product 6 for GC-FID analysis.

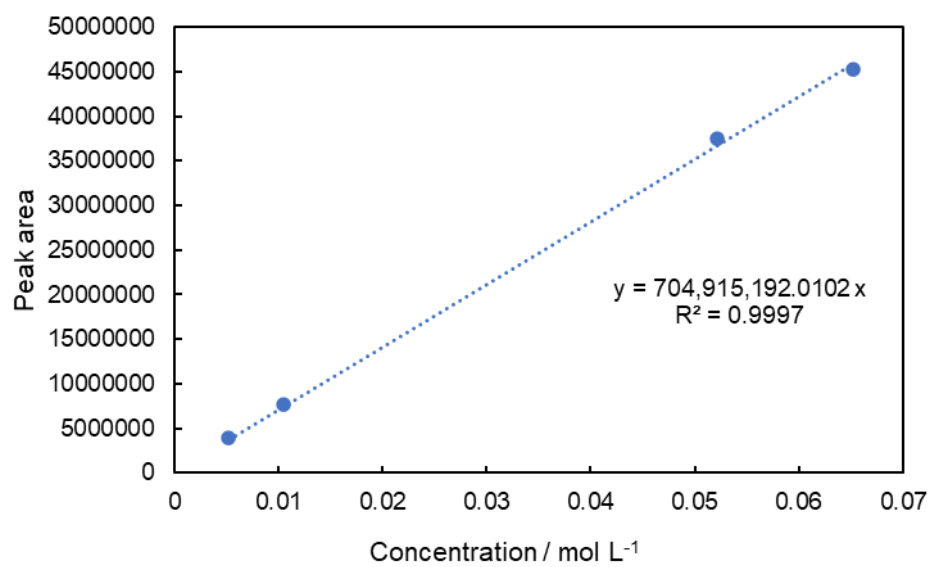


Fig. S24 Calibration curve of product **8** for GC-FID analysis.

20. ^1H NMR spectra

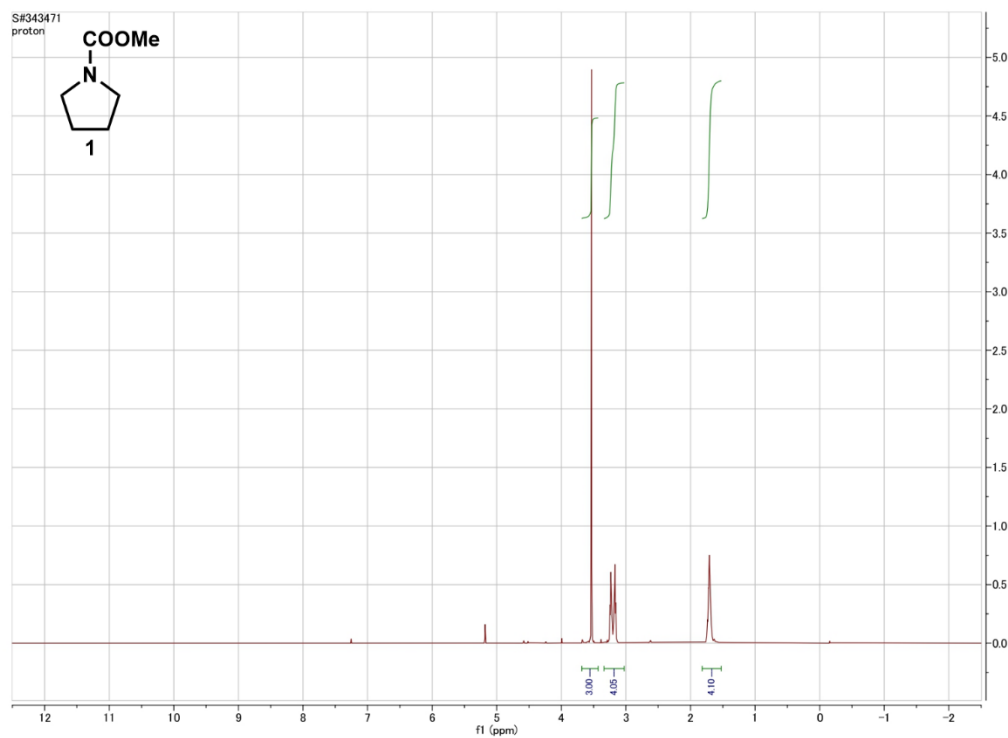


Fig. S25 ^1H NMR spectrum (500 MHz, CDCl_3 , 25 $^\circ\text{C}$) of 1.

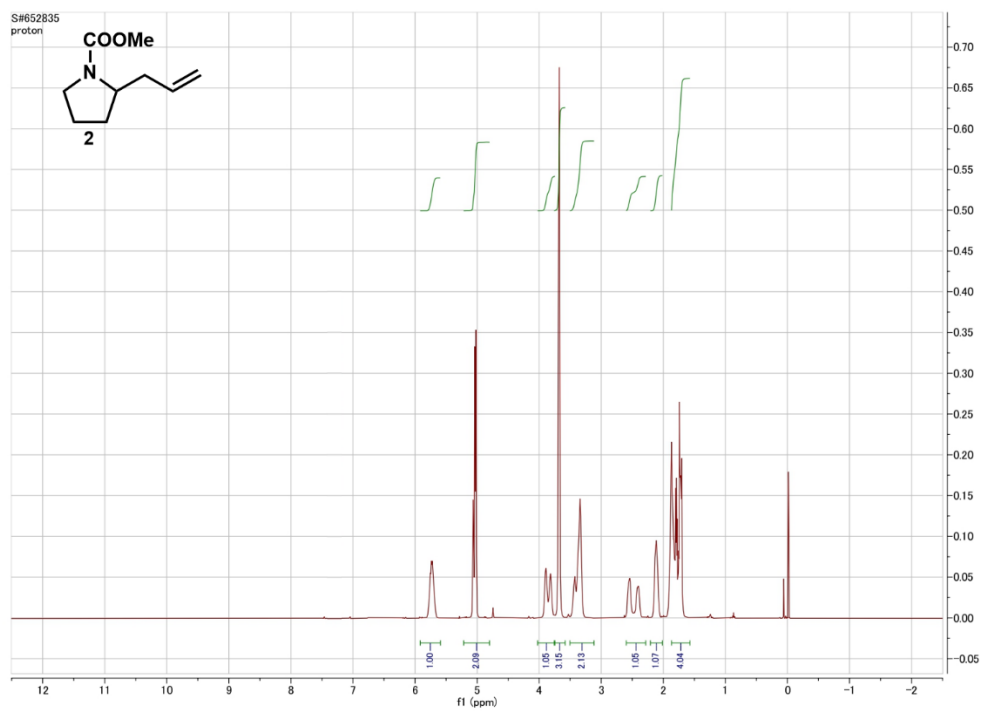


Fig. S26 ^1H NMR spectrum (500 MHz, CDCl_3 , 25 $^\circ\text{C}$) of 2.

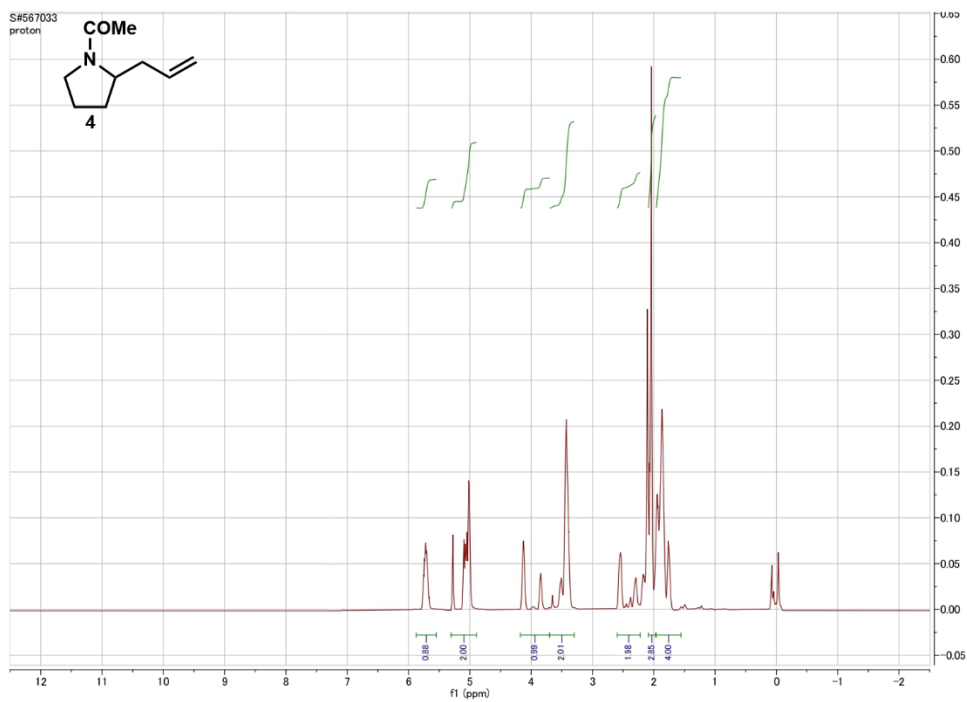


Fig. S27 ^1H NMR spectrum (500 MHz, CDCl_3 , 25 $^\circ\text{C}$) of **4**.

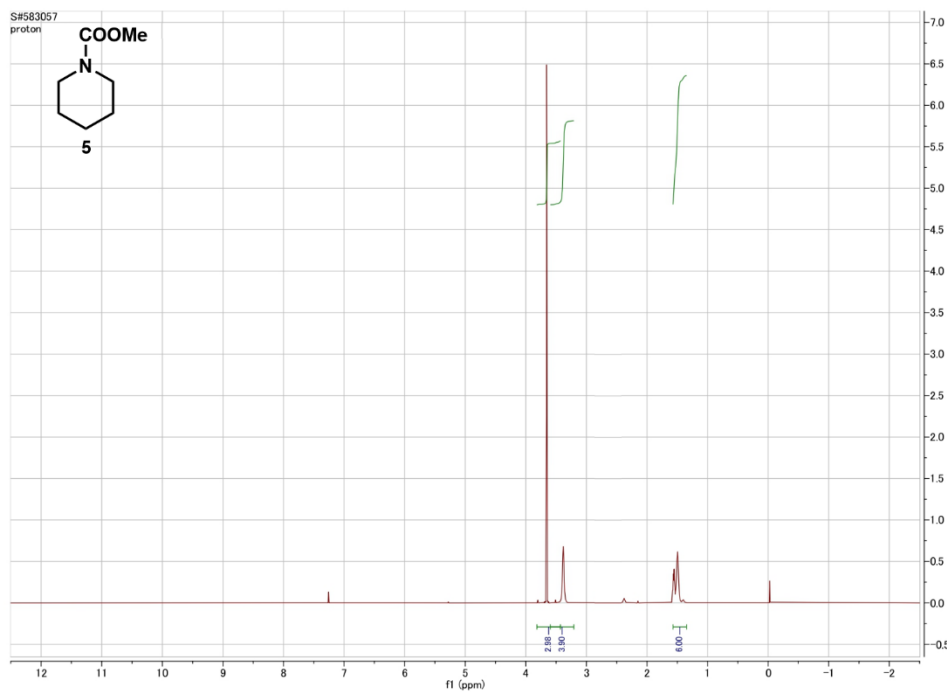


Fig. S28 ^1H NMR spectrum (500 MHz, CDCl_3 , 25 $^\circ\text{C}$) of **5**.

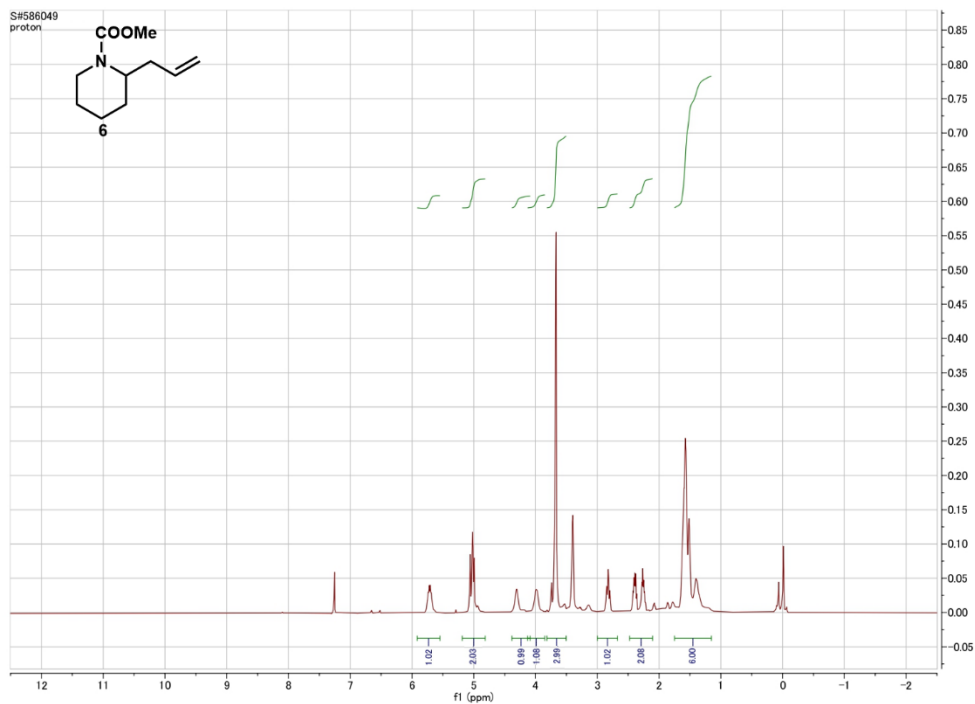


Fig. S29 ^1H NMR spectrum (500 MHz, CDCl_3 , 25 $^\circ\text{C}$) of **6**.

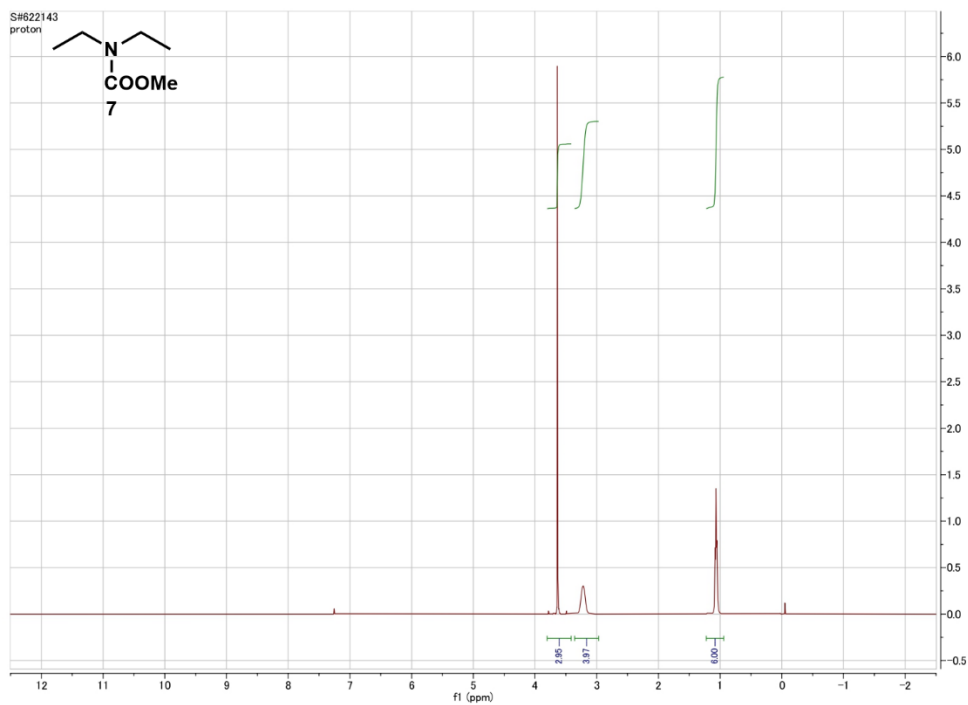


Fig. S30 ^1H NMR spectrum (500 MHz, CDCl_3 , 25 $^\circ\text{C}$) of **7**.

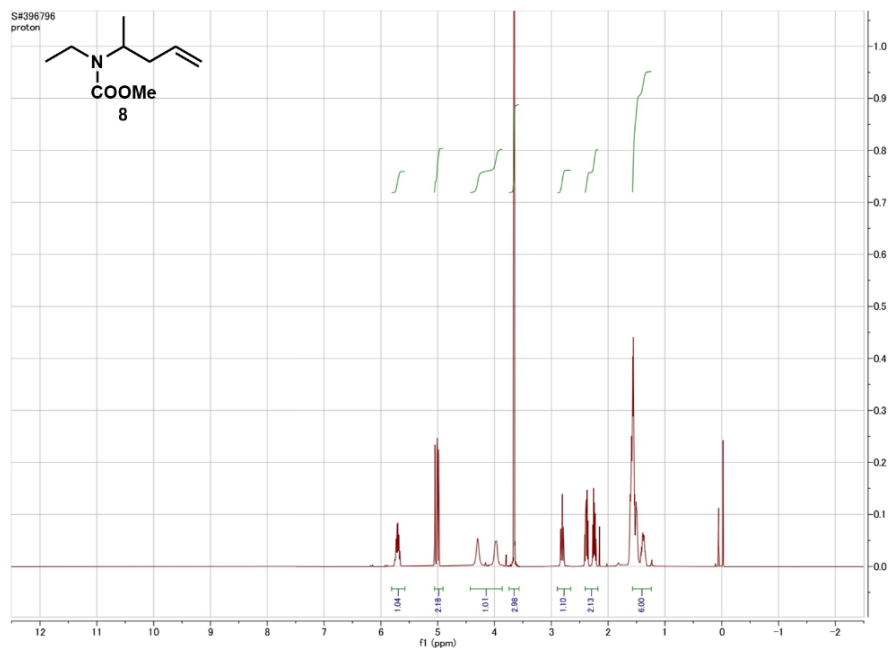


Fig. S31 ^1H NMR spectrum (500 MHz, CDCl_3 , 25 $^\circ\text{C}$) of **8**.

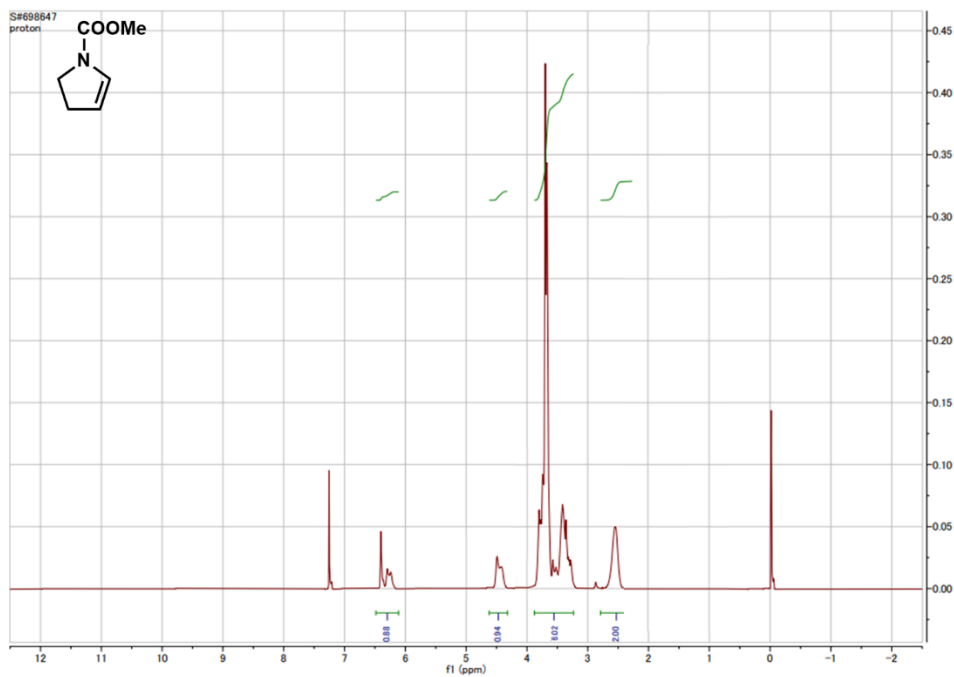


Fig. S32 ^1H NMR spectrum (500 MHz, CDCl_3 , 25 $^\circ\text{C}$) of the β -proton elimination product, *N*-(methoxycarbonyl) pyrroline.

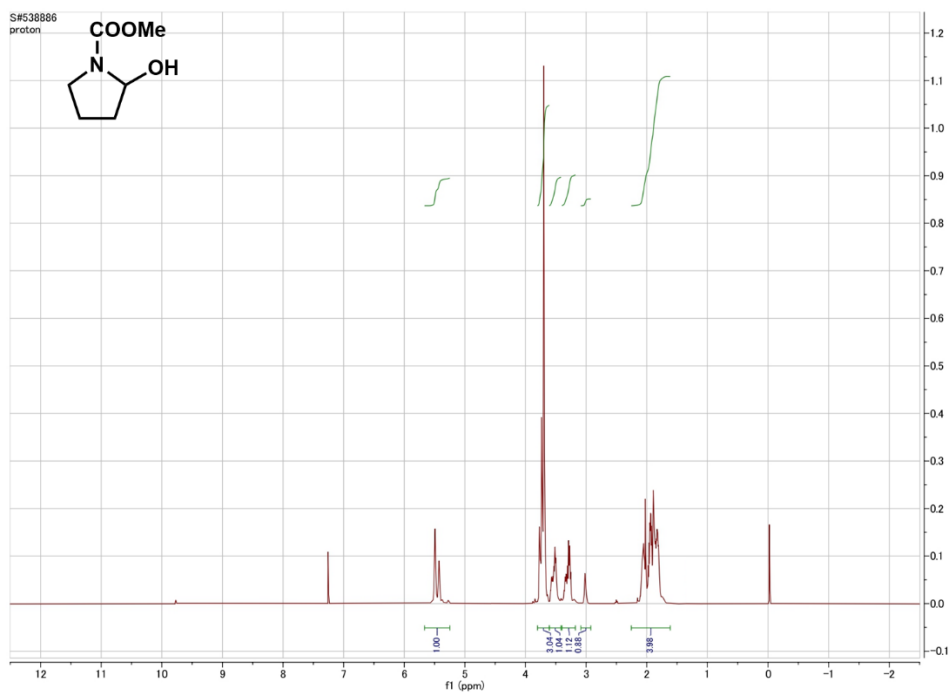


Fig. S33 ^1H NMR spectrum (500 MHz, CDCl_3 , 25 $^\circ\text{C}$) of the α -hydroxylated product, 2-hydroxy-*N*-(methoxycarbonyl)-pyrrolidine.

21. Supporting references

- 1 K. Fuchigami, T.; Matsumura, Y.; Tsubata, *Org. Synth.*, 1985, **63**, 206–211.
- 2 A. Boto, R. Hernández and E. Suárez, *J. Org. Chem.*, 2000, **65**, 4930–4937.
- 3 T. Shono, T.; Matsumura, Y.; Tsubata, K.; Sugihara, Y.; Yamane, S.; Kanazawa, T.; Aoki, *J. Am. Chem. Soc.*, 1982, **104**, 6697–6703.
- 4 M. Vargas-Sanchez, S. Lakhdar, F. Couty and G. Evano, *Org. Lett.*, 2006, **8**, 5501–5504.
- 5 K. Hayashi, K.; Kim, S.; Chiba, *Electrochemistry*, 2006, **74**, 621–624.
- 6 S. Ishii, H. Nakayama, Y. Yoshida and T. Yamashita, *Bull. Chem. Soc. Jpn.*, 1989, **62**, 455–458.
- 7 S. Suga, M. Okajima, K. Fujiwara and J. I. Yoshida, *QSAR Comb. Sci.*, 2005, **24**, 728–741.
- 8 D. K. Winter, A. Drouin, J. Lessard and C. Spino, *J. Org. Chem.*, 2010, **75**, 2610–2618.